Communications in Physics, Vol. 27, No. 4 (2017), pp. 301-310
DOI:10.15625/0868-3166/27/4/10752

EVOLUTION OF BORON NITRIDE STRUCTURE UPON HEATING

NGUYEN THI THUY HANG[†]
Ho Chi Minh City University of Technology, VNU – HCM, Vietnam

[†]*E-mail:* hangbk@hcmut.edu.vn

Received 23 September 2017
Accepted for publication 26 November 2017
Published 22 December 2017

Abstract. *The evolution of structure upon heating of hexagonal boron nitride nanoribbon (h-BNNR) model is studied via molecular dynamics simulation. The temperature is increased from 50 K to 5500 K in order to observe the change of the structure during heating process. Various thermodynamic quantities related to the change of structure are calculated such as the radial distribution functions the Lindemann criterion, the occurrence/growth of liquidlike atoms, the formation of clusters, and the ring statistics. The melting point is defined. The phase transition from solid to liquid states exhibits first order behavior.*

Keywords: melting of hexagonal boron nitride nanoribbon, melting criterion, phase transition, cluster.

Classification numbers: 81.07.Nb, 64.70.Na, 64.70.dj.

I. INTRODUCTION

Due to physical properties such as strong mechanical properties, high chemical and thermal stability of two-dimensional (2D) crystal [1, 2], different 2D materials are studied to apply for modern electronic devices [3–10]. Among these 2D materials, hexagonal boron nitride (h-BN) nanoribbon is studied widely because h-BN can be a suitable substrate for graphene due to the similar structure and the defect structure of h-BN can be used as molecular adsorption in graphene [11, 12]. There are many theoretical and experimental studies of h-BNNR. Freestanding single layer of h-BN has been studied experimentally [13] to observe the existence of monovacancies and the large vacancies with nitrogen atom at the zigzag edge. The energy of breaking bond or moving a nitrogen (N) atom are analyzed [14]. Moreover, h-BNNRs displayed semiconductor

materials in some conditions of the edges [15] and that can shed new light on h-BNNRs in production and usage as functional semiconductors with a wide range of applications in optoelectronics and spintronics. In addition, h-BN as well as BNNRs can be considered as one of the promising dielectric materials in hybrid graphene devices [16–18].

The heating process of h-BNNR is defined for the model with 50 atoms using the density functional theory (DFT) [19]. However, due to the limited size of the model of DFT, the melting point can be higher when the size of model increases. In an attempt to study the intermediate structures as well as the information on the phase transition at temperatures close to and exceeding the melting point of h-BNNR upon heating, we performed a detailed molecular dynamics study via various thermodynamic quantities related to the melting such as the radial distribution functions, the two-dimensional Lindemann criterion, occurrence/growth of liquidlike atoms and atomic mechanism of heating process. Details about the calculations are showed in Sec.II. Results and discussions related to the thermodynamics of h-BNNR upon heating can be found in Sec.III. Conclusions are given in the last section of the paper.

II. CALCULATION

In this study, we investigate the evolution upon heating of free standing h-BNNR by molecular dynamics (MD) simulations via a Tersoff potential which is parameterized by Albe *et al.* [20]

$$E_b = \frac{1}{2}\sum_{i\neq j} f_c\left(r_{ij}\right)\left[f_R\left(r_{ij}\right) + b_{ij} f_a\left(r_{ij}\right)\right],$$

where r_{ij} denotes the distance from atom i to atom j and the sum runs over all atomic sites. The repulsive $f_R(r_{ij})$ and the attractive $f_a(r_{ij})$ terms are chosen similar to a Morse potential as proposed by Brenner [21]. The $f_c(r_{ij})$ term represents a cutoff function, which calculate the number of neighbors and makes the potential to zero outside the interaction shell.

In order to perform the calculations we use the software package Large-Scale Atomic/Molecular Massively Parallel Simulator (LAMMPS), designed to solve various problems by the methods of classical molecular dynamics [22].

The initial crystalline h-BNNR model contains 10000 identical atoms of B and N in a rectangle of the size of $167.72 \times 167.163 \text{Å}^2$ under periodic boundary conditions (PBCs) have been relaxed in the isothermal-isobaric ensemble (NPT) for 3×10^5 MD steps at $T_0 = 50$ K. Note that 1 MD step takes 0.0001 picoseconds. In order to get the nanoribbon of h-BN the PBCs are applied only along the y Cartesian coordinates while along the x Cartesian coordinates the non-periodic boundary with an elastic reflection behavior is employed after adding the empty space of $\Delta x = 20$Å at both side $x = 0$ and $x = 167.72$Å. The system is left to equilibrium further for 2.10^5 MD steps at $T_0 = 50\ K$ using canonical ensemble simulation corresponding to the new boundaries of the simulation cell. Then the model is heated from 50 K to 5500 K to get all information on the phase transitions, intermediate structures at temperatures close to and exceeding the melting point of h-BNNR. The heating rate is 10^{12} K/s.

We employ the Interactive Structure Analysis of Amorphous and Crystalline Systems (ISAACS) software for calculating the ring statistics [23]. We use the Visual Molecular Dynamics (VMD) software (Illinois Univ.) for 2D visualization of atomic configurations [24]. For calculations of the rings, the 'shortest path' rule is applied [23]. Temperature of the system is increased linearly via velocity rescaling as follows: $T = T_0 + \gamma t$. Here, $T_0 = 50$ K and γ is a heating

rate, t is a time required for heating. Models, obtained at each temperature have been relaxed at a given temperature for 6×10^5 MD steps before analyzing the structural characteristics or 2D visualization.

III. RESULTS AND DISCUSSION

As well know that solids have regular, periodic structures, with molecules fluctuating near their lattice positions. Discrete peaks can be seen in the radial distribution functions (RDF) of a solid. Each peak has a broadened shape which is caused by particles vibrating around their lattice sites. There is zero probability of finding a particle in regions between these peaks as all molecules are packed regularly to fill the space most efficiently. However, upon heating the atoms gain enough energy to vibrate far from equilibrium positions leading to the formation of distorted structure, defects, and finally liquid state. In this study, the evolution of structure of h-BNNR is reflected via RDF upon heating to molten state (Fig. 1).

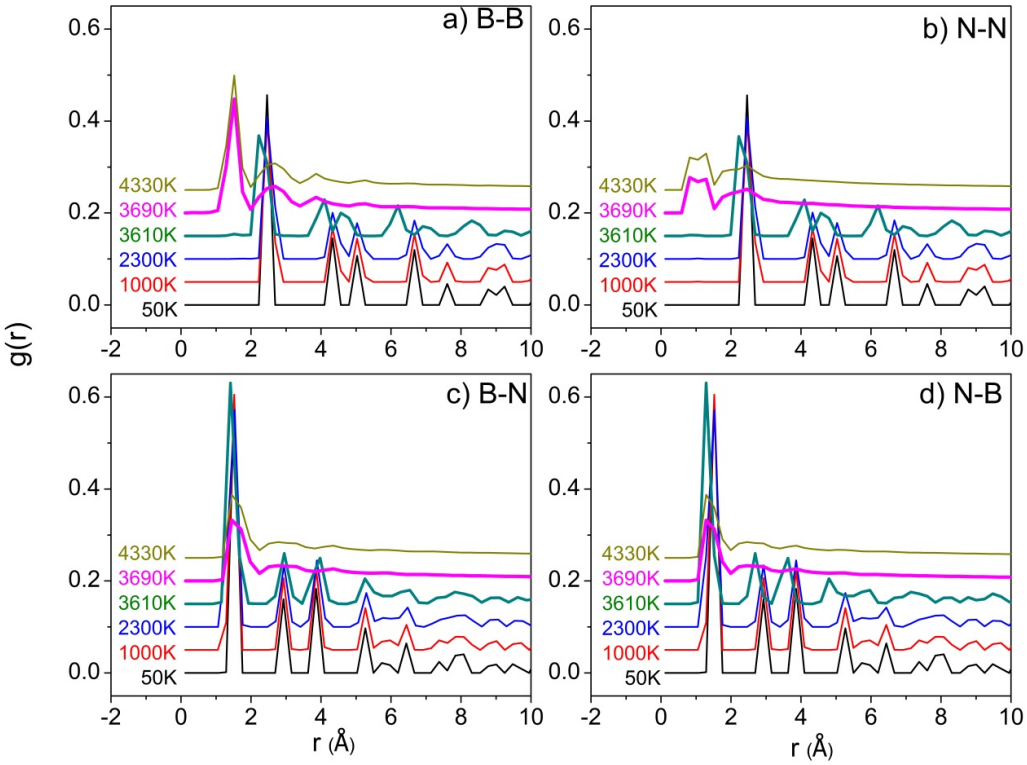

Fig. 1. Temperature dependence of RDF upon heating: a) B-B, b) N-N, c) B-N, d) N-B.

One can see that the behavior of the peaks in RDF lines decreases and becomes smooth with increasing temperature. In the range of temperature less than 3610 K, the RDFs exhibit crystalline structure of the model because they contain many peaks (Fig. 1). At temperature 3610 K, the change of peaks can be observed clearly for B-B and N-N cases (Figs. 1a,b) whereas it is not clear

change in B-N and N-B cases (Figs. 1c,d). However, upon heating to 3690 K, the behavior of the peaks is almost smooth at the distance further than first peak indicating liquid state. While the first peaks of B-N and N-B are slightly changed to the smaller distance (Figs. 1c,d), the ones of B-B and N-N (Figs. 1a,b) are significantly shifted to smaller distance indicating the ring formation and crystalline structure is washed out like that found in reference [25]. This behavior related to the formation of shorter bonds in the rings/clusters like that suggested in reference [25]. Note that in typical simple systems, the first peak shifts to a larger distance when it is going from crystal into liquid [26].

Upon heating, the energy per atom in the model increases and causes the collapse solid structure of whole model at the melting point. This process for present model upon heating from 50 K to 5500 K can be seen in Fig. 2.

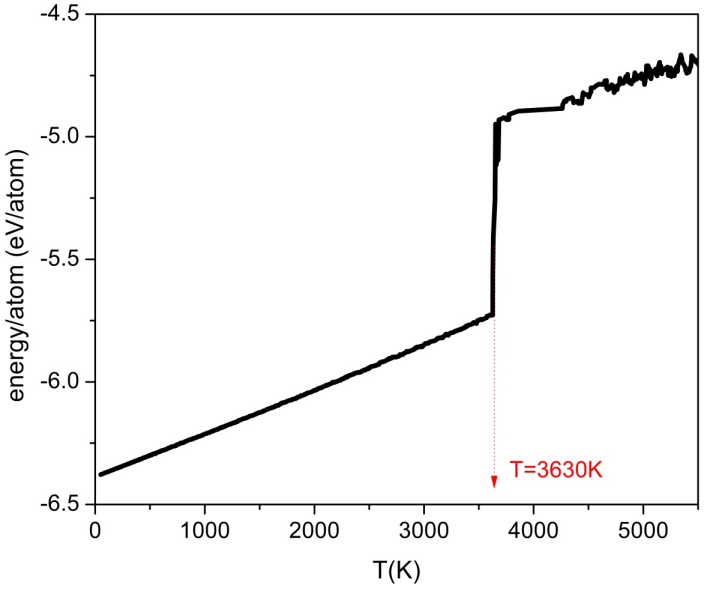

Fig. 2. Temperature dependence of total energy per atom.

It is clear from the graph that in the temperature range of 50 to 3360 K, total energy linearly increases with temperature since the system remains in solid state, and vibrational motion of atoms near their equilibrium positions dominates in the system. At temperature 3630 K the contribution of anharmonic motions of atoms is strong enough leading to a massive collapse of a crystalline matrix and the total energy starts to deviate from the linear law (Fig. 2). The total energy has a sharp increase at 3630 K exhibiting clearly a first order-like phase transition from solid to liquid states and $T = 3630$ K can be considered as melting point of the model. A temperature higher than 3630 K, the total energy increases linearly again indicating that the model is in liquid state.

Up to now, there has not been any experimental result about the melting point of h-BNNR. So that, the melting point of h-BN is taken to compare to the one of h-BNNR in this study because the h-BNNR (1D material) is created by fixing one dimension of h-BN (2D material). Therefore,

h-BNNR inhibits almost the h-BN's properties. The phase transition from h-BN to other forms is studied experimentally [27]. Gleiman et al. showed that the melting process of h-BN is occurred in the temperature range from 2800 K to 3600 K. The melting point of h-BNNR in this study $T = 3630$ K is a bit higher than that obtained in simulation [27] may be due to the fixing one dimension of h-BN to create h-BNNR.

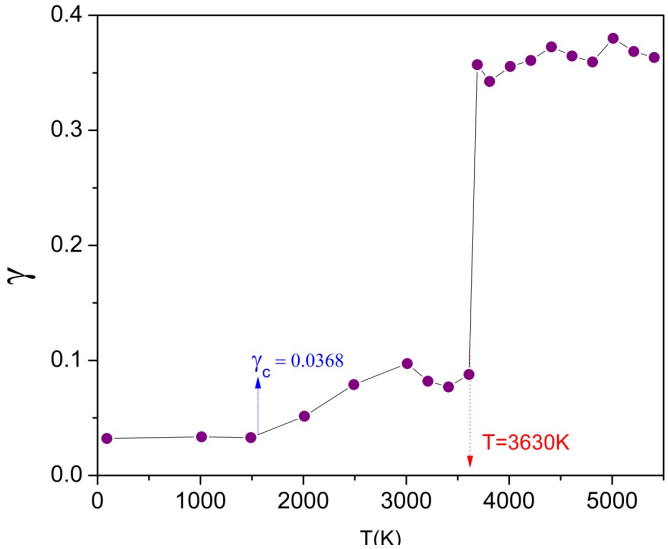

Fig. 3. Temperature dependence of average quantity for 3 atoms closest to *i-th* atom.

Atomic mechanism of melting process can be studied via the formation of liquid-like atoms defined by the Lindemann criterion. As is known that the Lindemann criterion shows that melting occurs because of vibrational instability, e.g. crystals melt when the average amplitude of thermal vibrations of atoms is relatively high compared with interatomic distances. In addition, the liquid-like atoms which cause the defects and distorted structure, or formation of clusters can be study using the Lindemann criterion. In 2D systems the mean square of the displacement $\langle u^2 \rangle$ is divergent at finite temperatures [28–30] leading to consider differences of atomic displacements [31]. Adapting the melting criterion used in Ref. [31] to the honeycomb lattice of h-BNNR the average quantity can be defined as follows:

$$\gamma_n = \frac{1}{a^2} \left\langle \left| r_i - \frac{1}{n} \sum_j r_j \right|^2 \right\rangle$$

where $a = 1/\sqrt{\pi\rho_0}$ and ρ_0 is the 2D particle density at $T = 0$ K, r_i is the position of the $i-th$ atom and where the sum over j runs over the n atoms closest to atom i. In present work, we show γ_n for $n = 3$, 9, and 12 atoms closest to $i-th$ atom.

Here we present the temperature dependence of the average quantity γ_3 for 3 atoms closest to *i-th* atom (Fig. 3). The graph of average quantity γ_3 starts to deviate from the linear law at $\gamma_3 = 0.0368$ and increases sharply at 3630 K. One can see that, the values of average quantity

$\gamma_3 = 0.0368$ can be considered as a critical value γ_C. Based on the critical value γ_C, atoms with $\gamma_n < \gamma_C$ are classified as solid-like atoms and with $\gamma_n > \gamma_C$ - liquid-like ones.

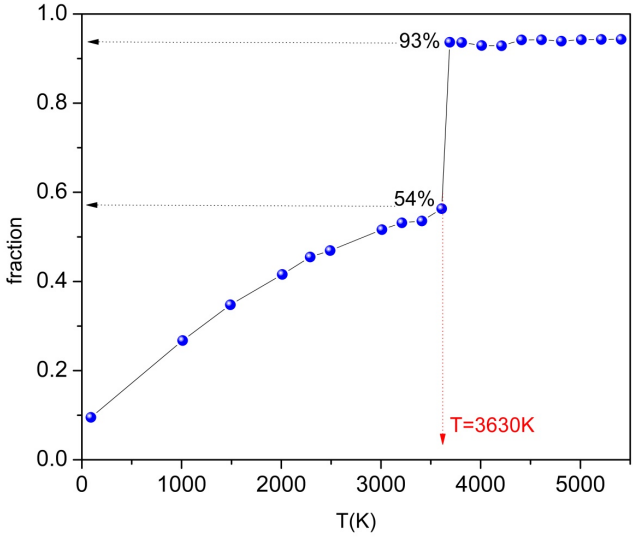

Fig. 4. Temperature dependence of the formation of liquid-like atoms.

The formation of liquid-like atoms upon heating based on the above Lindemann criterion $\gamma_C = 0.0368$ can be seen in Fig. 4. At temperature below the melting point (3630 K), the number of liquid-like atoms increases steady (about 56%), while there is a sharp increase at temperature just around 3630 K (about 93%) indicating that the phase transition from solid to liquid states takes place at temperature around 3630 K. In the range of temperature from 3630 K to 5500 K the number of liquid-like atoms remains constant (around 94%) exhibits the conclusion that in liquid state a tiny number of atoms in the model does not become liquid-like atoms. Note that the liquid-like atoms have tendency to form clusters. The change of maximal size of clusters upon heating can be seen in Fig. 5. Here, S_{max} is size of their maximal clusters and N is total number of atoms in model.

Temperature dependence of the formation of maximal cluster (Smax/N). Temperature dependence of the formation of maximal cluster (Smax/N). Looking at the graph of the formation of maximal cluster upon heating one can see that at temperature below 1500 K the size of maximal cluster increases steady, after that it rises sharply from temperature 1500 K to 2300 K. In the range of temperature from 2300 K to 3630 K the size slightly increases before having an incredible change at temperature of 3630 K. At temperature above 3630 K the size of maximal cluster fluctuates slightly and contains around 94% of liquid-like atoms indicating that the maximal size of cluster does not contain all atoms.

To study the distorted structure the angle distributions N-B-N and B-N-B are presented at different temperatures (Fig. 6). As is known that the solid structures show angle $\gamma \approx 120^\circ$ and distorted structures have angle $\gamma \neq 120^\circ$ between B-N-B or N-B-N.

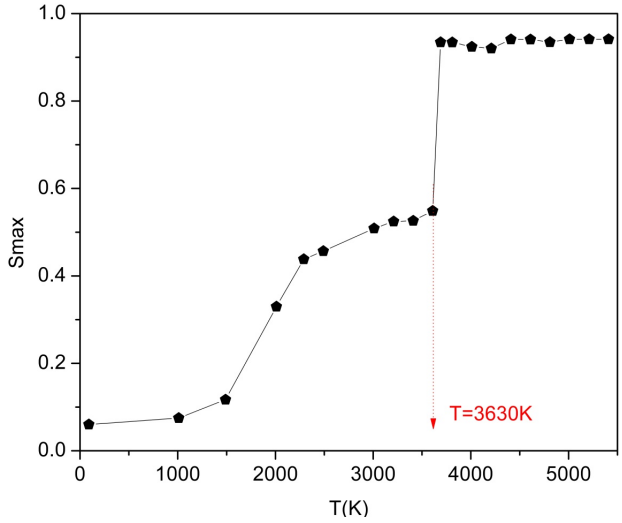

Fig. 5. Temperature dependence of the formation of maximal cluster (Smax/N).

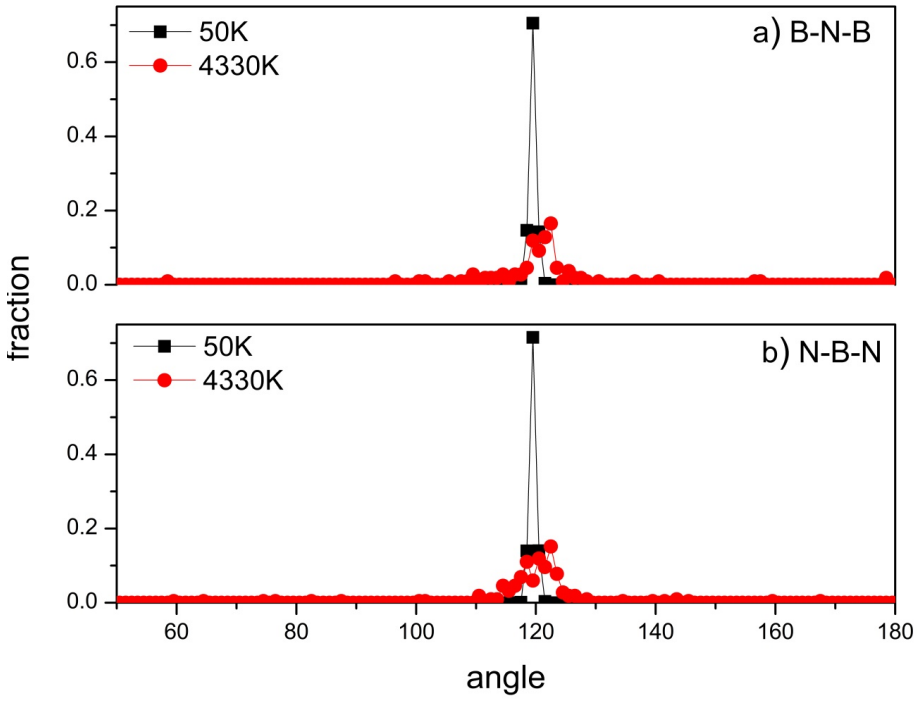

Fig. 6. Angle distributions at various temperatures of N-B-N.

At 50 K, the fractions of angle distributions of N-B-N and B-N-B distribute only in the narrow range of 120°– 123.1° indicating that the model is in solid state (square in Figs. 6a,b). At

temperature above the melting point, the fraction decreases significantly leading to the increase in distribution in the wide range of 90°– 145° (solid circle in Figs. 6a,b) indicating the existence of different distorted structures. This situation leads to the formation of various ring sizes which is analyzed below. Especially, the fraction of angle $\gamma \approx 120^{\circ}$ occupies a tiny percentage indicating that the model is in liquid state. More information about the change of structure upon heating h-BNNR can be based on the formation of ring distributions at various temperatures (Fig. 7).

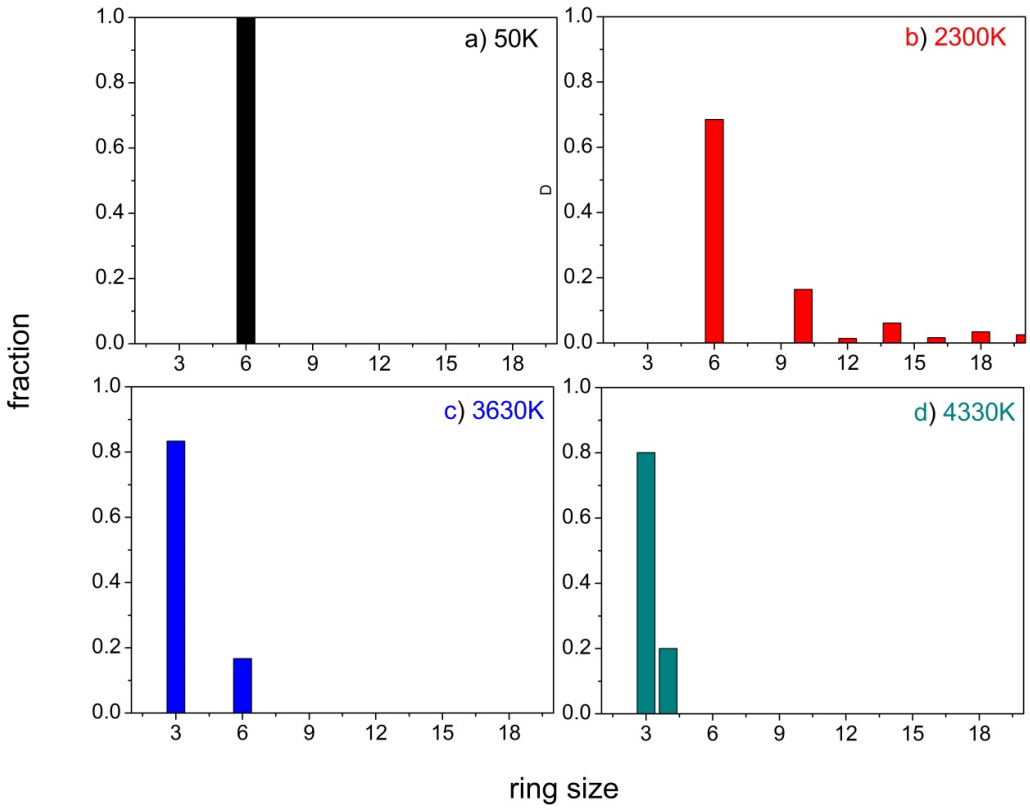

Fig. 7. Ring distributions at various temperatures.

At initial temperature (50 K) the mean ring size equals 6 indicating that the model remains in solid state with honeycomb structure (Fig. 7a). At temperature of 2300 K the fraction of non-6-fold rings ranged from 10-fold to 20-fold rings increases leading to the decrease in the fraction of 6-fold ring (Fig. 7b). Upon heating to the melting point (3630 K) there are only 3-fold and 6-fold rings. While the 3-fold ring reaches to the highest percentage (near 85%), the 6-fold ring sizes decreases sharply (near 15%) (Fig. 7c). In increase in temperature to higher melting point (4330 K), the 3-fold ring decreases slightly whereas the 6-fold ring disappears and the 4-fold ring forms. One can see that there are no any large ring sizes in liquid state and this behavior can be seen in 3D visualization. Note that the same model have been done for graphene nanoribbons and the results show that the large carbon chains are formed in liquid state.

Details of melting process can be seen via a side view of 3D visualization of occurrence of the liquid-like atoms in the system during the heating process (Fig. 8). At temperature of 50 K, the model is solid state (Fig. 8a). Upon heating, the liquid-like atoms occur first at the boundaries due to the local instability and liquid-like configuration grows/enhances gradually into the interior (Figs. 8b,c). At the melting point (3630 K), there is a collapse of the solid structure to form the liquid state and liquid-like atoms tend to form clusters (Fig. 8d).

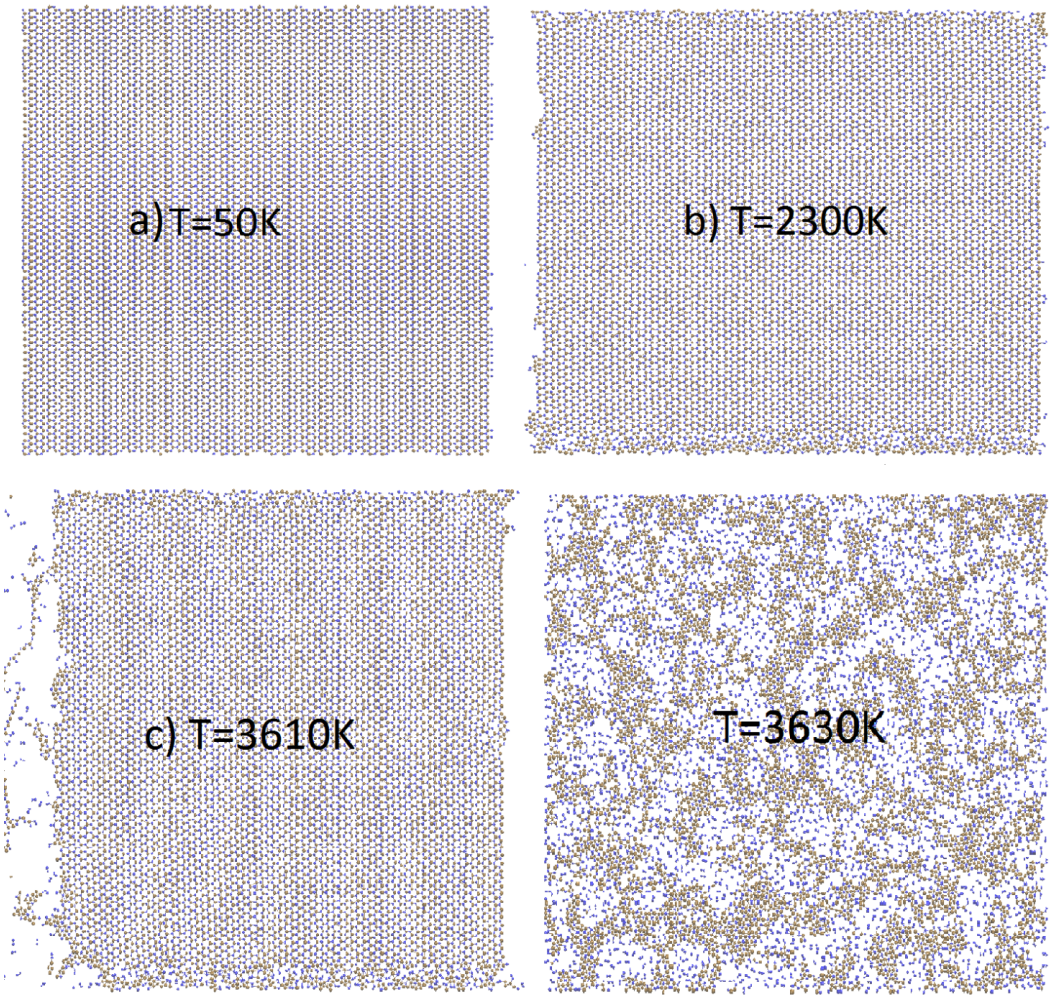

Fig. 8. A side view of 3D visualization of structure h-BNNR at different temperatures.

IV. CONCLUSIONS

We have carried out a comprehensive MD simulation of melting of h-BNNR model with a realistic Tersoff potential in 2D case to study the evolution of structure. The evolution of structure

is observed using the radial distribution functions. Unlike bulk materials, the first peaks of radial distribution functions shift to the smaller distance upon heating. The Lindemann criterion for 2D case $\gamma_{C3} = 0.0368$ is used to define the liquid-like atoms. Upon heating, the liquid-like atoms appear/grow first at the edges and then in the whole model at the melting point. Liquid-like atoms have a tendency to form clusters and the maximal size of cluster in liquid state contains near 94% of total atoms. In liquid state, there are no any large ring sizes. The phase transition exhibits first order behavior and melting point 3630 K is defined.

ACKNOWLEDGEMENTS

This research is funded by Ho Chi Minh City University of Technology – VNU-HCM under grant number T-KHUD-2017-37.

REFERENCES

[1] D. Jin-Xiang, Z. Xiao-Kang, Y. Qian, W. Xu-Yang, C. Guang-Hua, and H. De-Yan, *Chinese Phys. B* **18** (2009) 4013.
[2] C. Li, Y. Bando, C. Zhi, Y. Huang, and D. Golberg, *Nanotechnology* **20** (2009) 385707.
[3] K. Nakada, M. Fujita, G. Dresselhaus, and M.S. Dresselhaus, *Phys. Rev. B* **54** (1996) 17954.
[4] K.S. Novoselov, A.K. Geim, S. Morozov, D. Jiang, M. Katsnelson, I. Grigorieva, S. Dubonos, and A. Firsov, *Nature* **438** (2005) 197.
[5] Y.-W. Son, M.L. Cohen, and S.G. Louie, *Phys. Rev. Lett.* **97** (2006) 216803.
[6] Y. Zhang, Z. Jiang, J. Small, M. Purewal, Y.-W. Tan, M. Fazlollahi, J. Chudow, J. Jaszczak, H. Stormer, and P. Kim, *Phys. Rev. Lett.* **96** (2006) 136806.
[7] A.K. Geim and K.S. Novoselov, *Nature materials* **6** (2007) 183.
[8] M.Y. Han, B. Özyilmaz, Y. Zhang, and P. Kim, *Phys. Rev. Lett.* **98** (2007) 206805.
[9] I. Meric, M.Y. Han, A.F. Young, B. Ozyilmaz, P. Kim, and K.L. Shepard, *Nat. Nanotechnol.* **3** (2008) 654.
[10] W.L. Wang, S. Meng, and E. Kaxiras, *Nano Lett.* **8** (2008) 241.
[11] C.R. Dean, A.F. Young, I. Meric, C. Lee, L. Wang, S. Sorgenfrei, K. Watanabe, T. Taniguchi, P. Kim, and K.L. Shepard, *Nat. Nanotechnol.* **5** (2010) 722.
[12] B. Sanyal, O. Eriksson, U. Jansson, and H. Grennberg, *Phys. Rev. B* **79** (2009) 113409.
[13] C. Jin, F. Lin, K. Suenaga, and S. Iijima, *Phys. Rev. Lett.* **102** (2009) 195505.
[14] G. Slotman and A. Fasolino, *J. Phys.: Cond. Mat.* **25** (2012) 045009.
[15] H. Zeng, C. Zhi, Z. Zhang, X. Wei, X. Wang, W. Guo, Y. Bando, and D. Golberg, *Nano Lett.* **10** (2010) 5049.
[16] D. Golberg, Y. Bando, Y. Huang, T. Terao, M. Mitome, C. Tang, and C. Zhi, *ACS nano* **4** (2010) 2979.
[17] M.S. Bresnehan, M.J. Hollander, M. Wetherington, M. LaBella, K.A. Trumbull, R. Cavalero, D.W. Snyder, and J.A. Robinson, *ACS nano* **6** (2012) 5234.
[18] Z. Yu, M. Hu, C. Zhang, C. He, L. Sun, and J. Zhong, *J. Phys. Chem. C* **115** (2011) 10836.
[19] D.-H. Kim, H.-S. Kim, M.W. Song, S. Lee, and S.Y. Lee, *Nano Convergence* **4** (2017) 13.
[20] K. Albe, W. Möller, and K.-H. Heinig, *Radiat. Ef. Defect. S.* **141** (1997) 85.
[21] D.W. Brenner, *Phys. Rev. B* **42** (1990) 9458.
[22] S. Plimpton, *J. Comput. Phys.* **117** (1995) 1.
[23] S. Le Roux and V. Petkov, *J. Appl. Crystallogr.* **43** (2010) 181.
[24] W. Humphrey, A. Dalke, and K. Schulten, *J. Mol. Graphics* **14** (1996) 33.
[25] K. Zakharchenko, A. Fasolino, J. Los, and M. Katsnelson, *J. Phys.: Cond. Mat.* **23** (2011) 202202.
[26] N.H. March and M.P. Tosi, *Introduction to liquid state physics* (2002) World Scientific.
[27] S. Gleiman, C.-K. Chen, A. Datye, and J. Phillips, *Journal of materials science* **37** (2002) 3429.
[28] N.D. Mermin and H. Wagner, *Phys. Rev. Lett.* **17** (1966) 1133.
[29] N.D. Mermin, *Phys. Rev.* **176** (1968) 250.
[30] L.D. Landau and E.M. Lifshitz, *Course of theoretical physics*, Vol. 5 (2013) Elsevier.
[31] V. Bedanov, G. Gadiyak, and Y.E. Lozovik, *Phys. Lett. A* **109** (1985) 289.